UNSYS digital

Journal of Unmanned System Technology

Preliminary Efficiency Performance Analysis of Lift-based Fin in Low-speed Flow and Low-frequency Tail-beat Based on Numerical Simulation

Arie Sukma Jaya and Muljowidodo Kartidjo

Center for Unmanned System Studies, Institut Teknologi Bandung, Bandung, Indonesia

Abstract—The present work analyzed efficiency performance of lift-based fin by using numerical method of Computational Fluid Dynamics (CFD). The simulation models were generated three-dimensionally comprises of lift-based and oscillating drag-based fins. Horizontal profile of the lift-based fins was an airfoil of NACA0012 to form wing-like fins, while vertical profile of the fins were divided into rectangular, tapered, and lunate shapes. Both lift and oscillating drag based fins have a similar aspect ratio, AR = 4. Movements of the fins were categorized into two kinematic schemes of oscillating and radial-sculling. The present mechanism of radial-sculling, mostly in lift-based fin, divided the tail into an oscillating part and a wing-like fin, connected by a free-rotation joint. The fins were simulated in a constant low-frequency tail-beat of f = 1 s-1 in a range of low-speed flow from 0.1-1 overall length (L)/s. A robust optimization method of Generalized Reduced Gradient (GRG) was performed to obtain an optimum value of simulation results. It is shown that fin angle affects efficiency performance of the lift-based fin. For the present simulation models of lift-based fins, the overall optimum efficiency occurs at fin angle between 40o-60o. In the variation of vertical profile shapes, the lift-based fin with lunate shape has a higher optimum efficiency than rectangular and taper shapes. However, in lower flow velocity or higher Strouhal number, a highest efficiency was achieved by the rectangular shape. By comparing the kinematic mechanisms, the present work show that radial-sculling of lift-based fin has a superior efficiency than the oscillating mechanism of drag-based fin within the similar aspect ratio and oscillating properties. The efficiency performance can be related to the wake pattern behind the fin. The present study suggests the implementation of lift-based fin with radial-sculling kinematic scheme for the practical application in low-speed flow and low-frequency tail-beat environment.

Keywords—CFD, lift-based, shape, angle, radial-sculling, kinematics, fin propulsion, efficiency.

DOI: 10.21535/just.v5i1.964

I. INTRODUCTION

In recent years, many efforts have been established to enhance marine propulsion system by applying biomimetic approach. Fin propulsion of fishes is one most extensively studied in the underwater biomimetics as the fishes have been ecological dominants in aquatic habitats. Therefore, in the area of biorobotic Autonomous Underwater Vehicle (AUV), Ref. [1] identified that the fish-like robot was the early focus and fish-like swimming became one of the interesting research topics. Another reference of Ref. [2] indicated that over the past few decades a significant number of prototype devices with biomimetic marine propulsion systems have been developed with various motives and referred as a robotic fish. One of the promising applications of biomimetic approach is the enhancement of efficiency properties of underwater vehicle. More efficient propulsion systems would reduce the power requirements and thereby lengthen mission durations. The common underwater propulsor of screw propeller was not efficient mechanism in a small underwater vehicle, as reported in Ref. [3]. Efficiency of less than 70% of the screw propeller is indicated in Refs. [4-5]. Therefore, study on efficiency of natural underwater propulsion system, such as fin of fishes, could provide solution for efficiency enhancement of the underwater vehicle.

Thrust mechanisms of fin propulsion can be simplified into drag-based and lift-based. One of the main differences between the mechanisms is generation of thrust by the streamlined profile on the lift-based fin. By moving relatively to the flow, the lift-based fin generates thrust similar to those lift producing mechanism in wing. Higher degree of freedom of the fin, represents by the fin angle, effectively reduce the lateral moment to achieve higher propulsive efficiency. Ref. [6] reported that drag-based propulsion of aquatic animals has less than 33% of efficiency, while Refs. [5, 7] reported that lift-based fishes and marine mammals have a maximum value of efficiency that higher than 80%. In relation with Strouhal number, typical efficiency peaks for most of swimming fishes were near St = 0.3 as reported in Refs. [8-9].

The sculling motion of lift-based fin has been experimentally studied in Ref. [10]. The study indicated that 90% efficiency performance was achievable by the sculling propulsion. However, the study of sculling lift-based fin in low-speed flow and low-frequency tail-beat is relatively rare. The present preliminary study is concerned with the efficiency performance of the lift-based fin in low-speed flow and low-frequency tail-beat based on numerical simulation. The tail-beat mechanisms of the fin are divided into two kinematic schemes of oscillating and radial-sculling. The present work attempts to apply the concept of wing-like fin as the rectangular

Corresponding author: A.S. Jaya (e-mail: arie.sukmajaya@gmail.com)
This paper was submitted on May 29, 2017; revised on July 4, 2017; and accepted on August 7, 2017.

and taper vertical profiles were included in the simulations, beside the common analyzed profile of lunate shape. For the purpose of numerical simulations, the developed simulation models and schemes are presented in Section II. Simulation results and analysis are included in Section III. The concluding remarks of the present work are presented in Section IV.

II. Numerical Simulation

Efficiency performance of the lift-based fins in the present research was evaluated numerically by using Computational Fluid Dynamics (CFD) method. The method involved simulation models and numerical scheme. The optimum efficiency values for the purpose of parameter analysis were evaluated by using optimization scheme of Generalized Reduced Gradient (GRG).

A. Simulation Models

Simulation models of the lift-based and drag-based fins were generated three-dimensionally in SolidWorks2014 environment and can be seen in **Figure 1**. The overall profile of the design of a small underwater vehicle with fin propulsion can be seen in the top image of the **Figure 1**. The overall profile consists of a fixed body, oscillating connector, and a caudal fin. The middle images of the figure show the lift-based simulation models. The effects of shapes on efficiency performance were represented by the variation on vertical profiles of rectangular, taper, and lunate shapes. NACA0012 is the horizontal profile of the wing-like fins, following the previous work in Ref. [11]. Oscillating drag-based fins, as shown in the bottom images of the **Figure 1**, were generated for the purpose of efficiency comparison with variation in rear-shapes such as round, truncate, fork, and lunate, following the previous study in Ref. [12]. All simulations fin models were designed to have similar aspect ratio, AR = 4. The summary of geometrical parameters of the simulation models can be seen in **Table I**.

Table I Geometrical parameters of the models

Overall Profile	Components		Body, connector, fin
	Overall length (L) [m]		0.5
	Body length [m]		0.32
	Connector length [m]		0.13
	Fin chord at root [m]		0.05
Fin Profile	Lift-based	Vertical	Rectangular, taper, lunate
		Horizontal	NACA0012
	Oscillating fins	Rear-shapes	Round, truncate, fork, lunate
	Height [m]		0.15
	Aspect Ratio, AR		4

B. Numerical Scheme

Numerical simulations of the present work were performed in ANSYS Workbench15 environment. The simulations involved a coupling between transient-structural of ANSYS Mechanical and ANSYS CFX components to accommodate further analysis on the effect of material properties of fin. For the present efficiency performance analysis, only fin parts were simulated. Movements for oscillating and radial-sculling of the fins were performed in transient-structural component. The schematic of the kinematic mechanism of oscillating and radial-sculling of the fins can be seen in **Figure 2**.

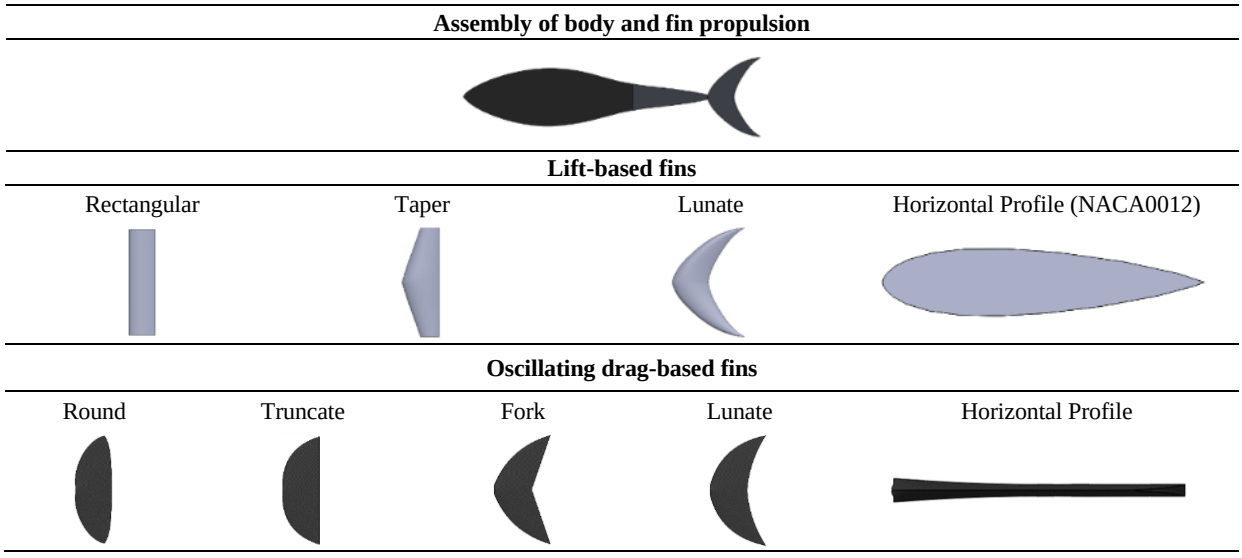

Figure 1 Profile of simulation model of fins

As shown in upper image of **Figure 2**, the oscillating motion was simply a radial oscillation of connector and fin to the center point O_1 with maximum oscillation angle θ_1. This motion produced by the oscillating drag-based mechanism. Another kinematic mechanism of radial-sculling, shown in lower image of **Figure 2**, uses two center points of O_1 and O_2

and two oscillation angles of θ_1 and θ_2. The oscillation angle of connector was fixed in all simulations at $\theta 1 = 20^o$. The fin angle, θ2, was defined from the centerline of the body and keeps constant along the fin motion. In real implementation, in order to keep a constant fin angle, a mechanical keeper system should be implemented at the center point of O_2.

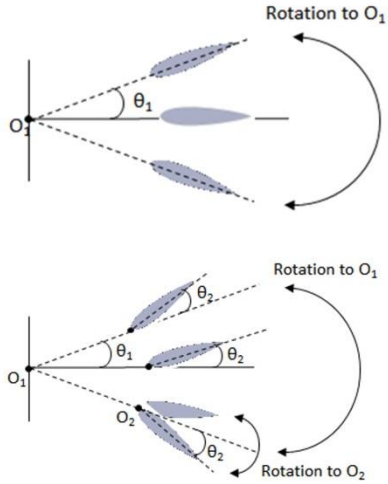

Figure 2 Kinematic mechanisms of fins: oscillating (upper), radial-sculling (lower)

The displacements results on transient-structural were transferred to the fluid analysis component through Fluid-Solid Interface scheme. A mesh convergence study was performed in order to balance simulation accuracy in fluid analysis with computing resources. The study involves several parameters such as mean thrust $\bar{T}$, mean lateral torque $\overline{Q_Y}$, and propulsive efficiency η. The efficiency was defined as the ratio between thrust power, P_T, to the lateral power, P_L, and can be expressed as

$$\eta = \frac{P_T}{P_L} \quad (1)$$

$$P_T = \bar{T} \times V \quad (2)$$

$$P_L = \overline{Q_Y} \times \omega \quad (3)$$

where V is the velocity of the fluid flow and ω is the angular velocity of the fin. The angular velocity of the fin was respect to the point of O_1 for both oscillating and radial-sculling.

TABLE II RESULTS OF MESH CONVERGENCE STUDY

No	Nodes	$\bar{T}$ [N]	$\overline{Q_Y}$ [Nm]	η [%]
1	52120	0.094	0.080	21.197
2	68760	0.085	0.076	20.036
3	105000	0.080	0.075	19.033
4	145046	0.078	0.075	18.517
5	180152	0.077	0.074	18.531
6	209522	0.077	0.074	18.663
7	224142	0.077	0.074	18.498

TABLE II shows the result of mesh convergence study of lift-based fins with lunate shape at flow velocity, V = 0.25 m/s (0.5 L/s), and motion frequency, f = 1 Hz. As indicated by the table, the results of mean thrust, mean lateral torque, and efficiency converged at the fourth scheme of nodes. Hence, the number of evaluated mesh for simulations in the present works was generated closely to this value. The unstructured tetrahedral mesh type was implemented for the simulations to accommodate higher degree of flexibility on mesh deformations. The sample of computational mesh and numerical scheme properties can be seen in **Figure 3** and **TABLE III**, respectively.

The size of computational domain in **Figure 3** was appropriate enough to observe flow phenomena of the model. Type of fluid in the present work is water, flowing uniformly from inlet to outlet. Relative pressure at outlet was set to 0 Pa. The unstructured mesh with inflation layers was implemented in the mesh generation in order to smoothly capture boundary layer on the body and propulsor surfaces. The k-omega SST was selected as the turbulence model to account for the transport of the turbulent shear stress in order to give an accurate prediction of the onset and the amount of flow separation.

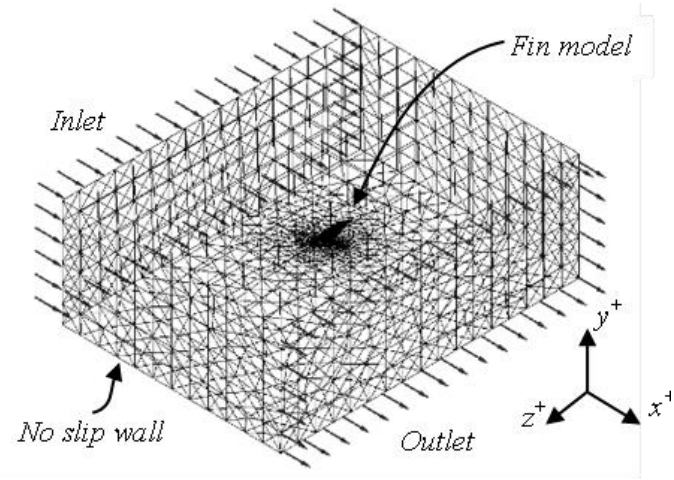

Figure 3 Computational mesh

TABLE III NUMERICAL SCHEME PROPERTIES

Numerical Analysis	ANSYS MultiField (Transient Structural and ANSYS CFX)
Computational Domain Size	Length: 14*c*, Width: 20*c*, Height: 12*c*. (*c* is the chord length of fins)
Symmetry plane	1 (ZX Plane)
Mesh Type	Unstructured Tetrahedral (72523 nodes on symmetry scheme)
Inflation Layer	10
Turbulence Model	Shear Stress Transport (Automatic Wall Function)
Transient Scheme	Second Order Backward Euler
Velocity	0.05 m/s - 0.5 m/s (0.1 L/s - 1 L/s)
Tail-beat frequency	1 Hz
Reynolds Number	2.8×10^3 - 2.8×10^4
Strouhal Number	0.2 – 1.95

Reynolds number in **TABLE III** describes the steady motion of the fin through the fluid. It is a dimensionless number that approximates the relative importance of forces due to the viscosity and inertia of fluid and can be expressed as

$$Re = \frac{\rho V c}{\mu} = \frac{V c}{v} \quad (4)$$

where ρ is the water density, V is the flow velocity, c is the chord length of the fin at the root, and μ and v are the dynamic and kinematic viscosity of the water, respectively. Another dimensionless number in Table III is the Strouhal number. The number represents the ratio of unsteady to inertial forces of the tail-beat motion and becomes parameter of the structure of wake behind the tail-beat. Strouhal number can be expressed as

$$St = \frac{2 h_0 f}{V} \quad (5)$$

where h_o is the tail-beat amplitude, f is the tail-beat frequency in Hertz, and V is the flow velocity. The further study of the optimum efficiency of the lift-based fins involved analysis on wake pattern. The wake pattern is represented by vorticity in which can be defined as a change of velocity vector in a space. Vorticity $\vec{\omega}$, can be expressed as

$$\vec{\omega} = \nabla \times \vec{v} \quad (6)$$

$$\vec{\omega} = \left(\frac{\partial v_z}{\partial y} - \frac{\partial v_y}{\partial z}, \frac{\partial v_x}{\partial z} - \frac{\partial v_z}{\partial x}, \frac{\partial v_y}{\partial x} - \frac{\partial v_x}{\partial y}\right) \quad (7)$$

where v_x, v_y, and v_z are the velocity components in x, y, and z space components, respectively.

C. Data Analysis and Optimum Value

All simulation data results were saved in the form in which can be transferred to the spreadsheet software such as Microsoft Excel. Data were analyzed in the worksheet and displayed as a graph for visualization purposes. Data analysis in Excel includes an optimization tool of Solver. The Solver finds an optimum value of an objective cell, which contains a function of data, by changing an input variable cell. In the present work, the function of data were generated by creating a polynomial regression line to a sampling data which has a value of coefficient of determination, $R^2 \approx 1$. The sampling data was selected from data near the initial maximum value of the data.

The solving method for the optimum value was Generalized Reduced Gradient (GRG) methods. As reported in Refs. [13-14], the GRG methods contain algorithms for solving nonlinear programs of general structure. In most application of the Solver in the present work was to find a maximum value of a function:

$$\text{Maximize objective function, } f(X) \quad (8)$$

$$\text{Subject to target function } g_i(X) = 0,\ i = 1, \ldots, m \quad (9)$$

$$l_i \le X_i \le u_i,\ i = 1, \ldots, n \quad (10)$$

where X is n-vector, li is lower bound, and ui is upper bound. The fundamental idea of GRG is to use the equalities in Equation (9) to express m number of basic variables in terms of the remaining n-m non-basic variables. The GRG code involved a variant of Newton method with the tolerance value for the convergence constrain was 0.0001.

III. RESULTS AND DISCUSSION

A. Effects of Fin Angle

Fin angle variation differentiates between oscillating and radial-sculling mechanisms. Fin angle represents the increasing of degree of freedom of motion of the fin propulsor. Hence, variation on fin angle can be related to the stiffness effect of the lift-based fins without considering material properties. The simulation results of the effect of fin angle to the efficiency performance at various Strouhal number can be seen in **Figure 4**. Zero fin angle, $\theta_2 = 0^o$, represents the oscillating fin.

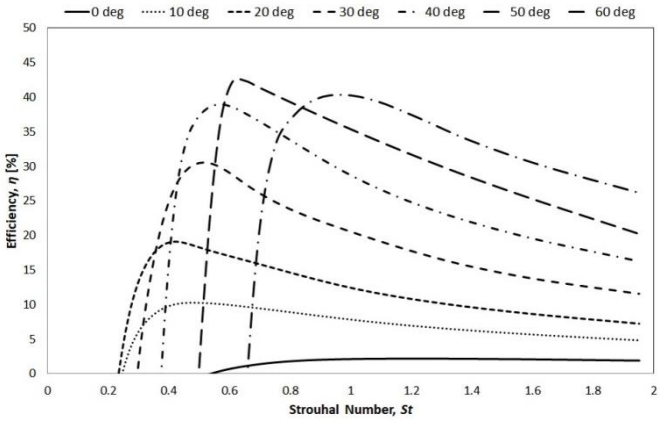

Figure 4 Effect of fin angle, θ_2, on efficiency performance

As shown in **Figure 4**, the fin angle affects efficiency performance of the lift-based fin. The maximum operating flow velocity of the lift-based fins represented by the overall minimum Strouhal number, which is around St = 0.24 (Vmax = 0.41 m/s or 0.82 L/s). On each fin angle configuration, there is a maximum efficiency with related Strouhal number. Up to θ2 = 50o, the maximum value of efficiency is shifted and increasing towards higher Strouhal number as the fin angle is increasing. However, the maximum efficiency decreases at θ2 = 60o, in which indicated that the optimum fin angle for the lift-based configuration in the present research is between 40o-60o. Higher fin angle has a narrower range of operating speed, as a negative efficiency occurs in low Strouhal number. The results also indicate that in lower flow velocity, represented by the higher Strouhal number, increasing fin angle increases efficiency of the fin propulsion.

B. Effects of Vertical Profile

Another parameter investigated in the present work is the effects of fin-shape to the efficiency performance. Variation of the vertical profile of the lift-based fin into rectangular, taper, and lunate shapes, could be focused for further enhancements in efficiency of fin propulsion. Efficiency performance on various shapes of the lift-based fins is presented in **Figure 5**. The simulation results were taken from the configuration of radial-sculling with fin angle, θ2 = 20o, due to its broader range of operating Strouhal number. The simulation result in **Figure**

5 clearly shows that vertical profiles of the lift-based fin affect the efficiency performance. The highest optimum efficiency on the present configurations is achieved by the lunate shape. The optimum value of lunate shape occurs in lower Strouhal number, thus at higher flow velocity, than rectangular and taper shapes. Hence, the result indicates that in order to achieve optimum condition, lunate shape should be implemented in high-speed flow regime, while rectangular shape should be preferred in low-speed flow regime.

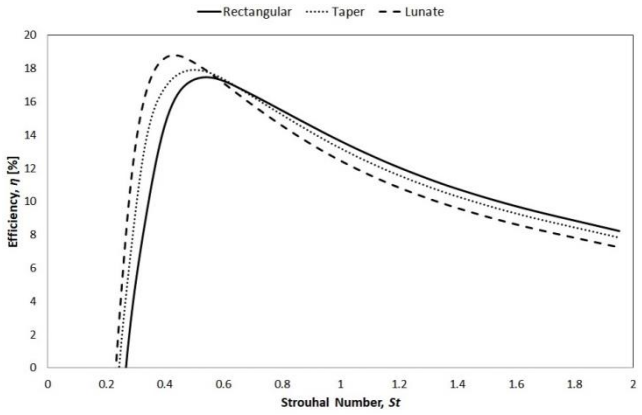

Figure 5 Effect of vertical profile shapes on efficiency performance at fin angle, $\theta_2 = 20^o$

TABLE III OPTIMUM EFFICIENCY PERFORMANCE AT FIN ANGLE, $\theta_2=20^O$

Vertical Profile	η_{opt} [%]	St_{opt}	St_{min}	(St_{min}/St_{opt}) [%]
Rectangular	17.483	0.541	0.266	49.190
Taper	17.922	0.500	0.243	48.682
Lunate	18.814	0.432	0.232	53.735

By using the optimization scheme in the present work, the optimum efficiency performance can be tabulated as in **TABLE IV**. The optimum values of Strouhal number in the present study are relatively higher than St = 0.3 as in Refs. [8-9]. Simulation on the fin part without body might be the possible cause of the higher optimum Strouhal number, since the previous studies were involved whole body part of fish or robotic fish. The values of Stmin represent the cruising speed of the fin. At relatively low-frequency tail-beat, within similar fin angle, lunate shape is able to achieve faster cruising speed than other vertical profiles. The result indicates that in cruising mode on low-frequency tail-beat, lunate shape produced higher thrust than other shapes. Another important consideration for fin propulsion operating condition is the ratio between minimum and optimum Strouhal number (Stmin/Stopt). The present results indicate that the lift-based fins reach the optimum efficiency at nearly twice of the cruising Strouhal number or half of the cruising speed. Hence, in order to maintain the efficient state of the fin propulsion within a constant tail-beat amplitude, forward speed and tail-beat frequency should be balanced to the required twice of the cruising Strouhal number.

C. Wake Pattern

Condition of the optimum efficiency can be compared to the sub-optimum configuration through wake pattern as shown in **Figure 6**. The wake pattern is represented by the vorticity contours behind the fin. The typical vorticity analysis is following previous study on efficient anguilliform swimming in Ref. [15]. Red and blue colored area represents the counter-clockwise and clockwise vortices, respectively. In the terms of thrust and lateral moment of the configurations, the generated thrust decreases as the decreasing of Strouhal number, while lateral moment increases with the decreasing of Strouhal number. The condition of high thrust with low lateral moment provided by the fin at high Strouhal number, as in the right image of the **Figure 6**. High thrust can be represented by large area and less separate red vortex, while large area and less separate blue vortex represents a low lateral moment condition. As the increasing of flow velocity, red vortex shifts farther from the fin and smaller area of blue vortex, thus reducing thrust and increasing lateral moment, as shown in the center and left images of the figure. The center image provides a condition of the optimum red and blue vortices orientation at the flow velocity about half of the cruising velocity.

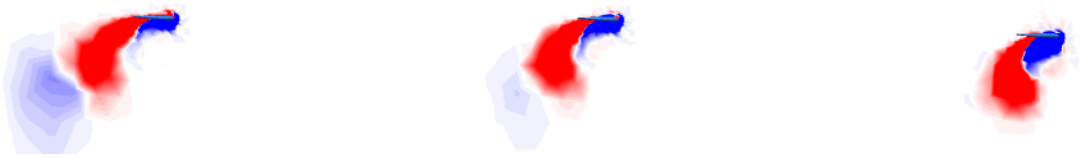

(a) **(b)** **(c)**

Figure 6 Vorticity-Y components, $|\omega_Y| = 1\ s^{-1}$, in a root plane of a lunate profile: (a) Sub-optimum, $St = 0.28$, (b) Optimum efficiency, $St = 0.43$, (c) Sub-optimum, $St = 1.3$. (Blue: negative vorticity, Red: positive vorticity)

Figure 7 Vorticity-Y components, $|\omega_Y| = 1\ s^{-1}$, in a root plane and $St = 1.95$: lunate profile (left), rectangular profile (right). (Blue: negative vorticity, Red: positive vorticity)

As shown in **Figure 5**, the efficiency performance of lunate shape is lower than other shapes in higher Strouhal number. The result on thrust and lateral moment of rectangular shape at St = 1.95 shows a decreasing thrust by 19% and lateral moment by 28% compared to the lunate shape. Hence, the reduction of input power component, which is higher than reduction in output power component, contributes to the higher efficiency of rectangular shape in low speed flow. The large reduction in lateral moment component can be observed on the wake pattern behind the lunate and rectangular shapes, as shown in **Figure 7**. The blue vortex of the rectangular shape, as in the right image of the figure, has a larger area than blue vortex in lunate shape. As the blue vortex has a similar orientation with fin motion, the large area of blue vortex indicates a lower resistance for the vortex creation, thus a lower power needed for the motion.

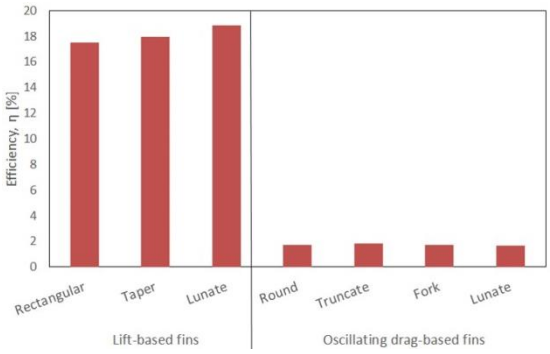

Figure 8 Optimum efficiency of lift-based fins and oscillating drag-based fins

D. Comparison to Oscillating Drag-Based Fin

The efficiency performance results of the lift-based fins can be compared to the oscillating drag-based fins. **Figure 8** shows the optimum efficiency comparison of the oscillating drag-based fins with various rear-shapes and lift-based fin with fin angle, $\theta_2 = 20^o$. As shown in the figure, all lift-based fins have a superior efficiency performance than the present configuration of oscillating drag-based fins. The smaller surface area of the drag-based fins in the present models, compared to the models in Ref. [12], is related to the lower thrust production of the fins. Furthermore, the differences in lateral moment of the two fin types are relatively low, thus contributes to the significant performance enhancement by the lift-based fins. The comparison result suggests that lift-based fins should be implemented for efficient fin propulsion.

IV. CONCLUSION

Numerical simulations have been performed to study the efficiency performance of lift-based fin. The radial-sculling mechanism increases degree of freedom of the kinematic motion of the fin. Fin angle of the radial-sculling motion represents the stiffness effect without concerning material properties of the fin, in which a higher fin angle indicates a lower stiffness of the fin. Fin angle of the radial-sculling mechanism affects the efficiency performance of the fin. Fin angle affects the maximum operating flow velocity of the lift-based fin, in which for the present configuration Vmax = 0.41 m/s (0.82 L/s). The optimum fin angle for efficiency of the lift-based fin is between 40o-60o. Lift-based fin in low-speed flow regime should implement a higher degree of fin angle to maintain the efficiency performance. On the effect of profile shape, lunate shape has a highest optimum efficiency than rectangular and taper shapes. Flow velocity for the optimum efficiency occurs at nearly 50% of the cruising flow velocity. In low-speed flow regime, rectangular shape should be preferred to obtain a relatively high efficiency. Wake pattern in the term of vorticity can be used to analyze and enhanced efficiency performance of the lift-based fin.

ACKNOWLEDGMENT

The authors would like to acknowledge the support of Center for Unmanned System Studies (CentrUMS-ITB). The first author gratefully acknowledges the support from Indonesia Endowment Fund for Education (LPDP).

REFERENCES

[1] W. Zhao, Y. Hu, and L. Wang, "Construction and Central Pattern Generator-Based Control of a Flipper-Actuated Turtle-Like Underwater Robot," Advanced Robotics 23, 19-43, 1999. CrossRef

[2] D.T. Roper, "Energy Based Control System Designs for Underactuated Robot Fish Propulsion", Ph.D. Dissertation, University of Plymouth, 2013.

[3] D. Mohammadshahi, A. Yousefi-Koma, S. Bahmanyar, H. Maleki, "Design, Fabrication and Hydrodynamic Analysis of a Biomimetic Robot Fish", Proceedings Mathematics and Computers in Science and Engineering, World Scientific and Engineering Academy and Society, 2008.

[4] S.F. Masoomi, S. Gutschmidt, X. Chen, and M. Sellier, "The Kinematics and Dynamics of Undulatory Motion of a Tuna-mimetic Robot", International Journal of Advanced Robotics Systems 12, 83, 2013. CrossRef

[5] F.E. Fish, "Advantages of natural propulsive systems", Mar. Technol. Soc. J., 47, 37-44, 2013. CrossRef

[6] F.E. Fish, "Transitions from drag-based to lift-based propulsion in mammalian swimming", Amer. Zool, 36:628-641, 1996. CrossRef

[7] P.W. Webb and P.T. Kostecki, "The effect of size and swimming speed locomotor kinematics of rainbow trout", Journal of Experimental Biology 109, 77-95, 1984.

[8] J.M. Anderson, K. Streitlien, D.S. Barrett, and M.S. Triantafyllou, "Oscillating foils of high propulsive efficiency", J. Fluid Mech., vol.360, pp. 41-72, 1998. CrossRef

[9] G.V. Lauder and E.D. Tytell, "Hydrodynamics of undulatory propulsion", Fish Biomechanics, Vol. 23, 425-468, 2006. CrossRef

[10] R.M.R. Muijtjens, "On the verification of a theory for sculling propulsion", Ph.D. Dissertation, Technische Universiteit Eindhoven, 1992.

[11] D.B. Quinn, G.V. Lauder and A.J. Smits, "Maximizing the efficiency of a flexible propulsor using experimental optimization", J. Fluid Mech., vol. 767, pp. 430-448, 2015. CrossRef

[12] A.S. Jaya and M. Kartidjo, "Preliminary numerical analysis of the effect of rear-fin shape on the oscillating propulsion performance", Marine and Underwater Science and Technology, Vol. 1, No. 2, 2015.

[13] L.S. Lasdon, R. Fox and M. Ratner, "Nonlinear optimization using the Generalized Reduced Gradient method", Tech. Memo. No. 325, Department of Operations Research, Case Western Reserve University, October 1973.

[14] L.S. Lasdon, A.D. Waren, A. Jain, M.W. Ratner, "Design and testing of a Generalized Reduced Gradient code for nonlinear optimization", Tech. Memo. No. 353, Department of Operations Research, Case Western Reserve University, October 1975.

[15] Stefan Kern and Petros Koumoutsakos, "Simulations of optimized anguiliform swimming," Journal of Experimental Biology 209, 4841-4857, 2006. CrossRef